

# System modeling based measurement error analysis of digital sun sensors

WEI Minsong<sup>1,2,3</sup>, XING Fei<sup>1,2,3,\*</sup>, WANG Geng<sup>1,2,3</sup>, YOU Zheng<sup>1,2,3</sup>

(1. Department of Precision Instrument, Tsinghua University, Beijing 100084, China;

2. State Key Laboratory of Precision Measurement Technology and Instruments, Tsinghua University, Beijing 100084, China;

3. Collaborative Innovation Center for Micro/Nano Fabrication, Device and System, Tsinghua University, Beijing 100084, China)

**Abstract:** Stringent attitude determination accuracy is required for the development of the advanced space technologies and thus the accuracy improvement of digital sun sensors is necessary. In this paper, we presented a proposal for measurement error analysis of a digital sun sensor. A system modeling including three different error sources was built and employed for system error analysis. Numerical simulations were also conducted to study the measurement error introduced by different sources of error. Based on our model and study, the system errors from different error sources are coupled and the system calibration should be elaborately designed to realize a digital sun sensor with extra-high accuracy.

**Key words:** digital sun sensors, measurement error, system modeling, numerical simulation

## 1 Introduction

The Digital Sun Sensor (DSS) is one of the most important sensors for the attitude measurement of the satellites<sup>[1-3]</sup>. With the advantages of the remote sensing and solar observation, a DSS with high accurate is required<sup>[4-5]</sup> and therefore, the measurement error of a DSS should be thoroughly studied for system calibration.

The measurement of incident sun angles is primarily implemented through the mask and the image detector (CCD or CMOS) of a DSS and by analyzing the location of the sun spot on image detector plane, the sun angles ( $\alpha$ ,  $\beta$ ) can be calculated through equations which are deduced from a simplified model<sup>[6-7]</sup>. To achieve a DSS with high accuracy, several different methods have been proposed and applied for DSS calibration and error compensation<sup>[8-10]</sup>. However, those methods usually focused on one or some parts of the sources of error and none of them studied the system measurement error based on a theoretical model of a DSS, especially including the refraction error.

In this work, we introduced a method to ana-

lyze the measurement error with respect to different error sources and based on our research, there are three different error sources including intrinsic parameter error, extrinsic parameter error and refraction error. The system error has been modeled based on the principle of a DSS and numerical simulations were conducted to analyze the measurement error with respect to different error sources, as well.

## 2 System modeling for error analysis of digital sun sensors

### 2.1 The rotation matrix

If coordinate  $X_1 Y_1 Z_1$  is rotated from coordinate  $X_0 Y_0 Z_0$  by the order of  $zxy$  with the angle parameter of  $(\theta_1, \theta_2, \theta_3)$ , the rotation matrix would be  $C_{10}$ :

$$C_{10} = \begin{bmatrix} C_2 C_3 - S_1 S_2 S_3 & -C_2 S_3 + S_1 S_2 C_3 & C_1 S_2 \\ C_1 S_3 & C_1 C_3 & -S_1 \\ S_1 C_2 + S_1 C_2 S_3 & S_2 S_3 - S_1 C_2 C_3 & C_1 C_2 \end{bmatrix} \quad (1)$$

Where,  $S$  demotes sine,  $C$  denotes cosine, and the subscript 1, 2, 3 denote the angle  $\theta_1, \theta_2, \theta_3$ , respectively.

### 2.2 System modeling for DSS error analysis

Fig. 1 reveals the relation between different co-

ordinates when a DSS is tested on a rotary table. Coordinate  $X_b Y_b Z_b$  is fixed in the center of the image detector of the DSS and coordinate  $X_a Y_a Z_a$  indicates the initial direction of three axes of the rotary table.

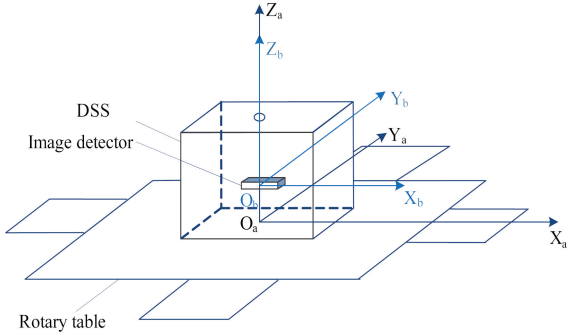


**Fig. 1** Schematic of DSS measurement on a rotary table

The two sun angles are both  $0^\circ$  when the rotary table is at its initial status and the incident sun vector can be expressed as  $\vec{S} = (0, 0, -1)$  in coordinate  $X_a Y_a Z_a$ . If coordinate  $X_c Y_c Z_c$  indicates the current direction of three axes of the rotary table after the rotary table is rotated from its initial status by the order of  $zxy$  with the angle parameter of  $(b_1, b_2, b_3)$ , the incident sun vector in coordinate  $X_c Y_c Z_c$  can be expressed as follows:

$$\vec{S}' = C_{ca} \vec{S} = \begin{bmatrix} \cos(b_1) \sin(b_2) \\ -\sin(b_1) \\ \cos(b_1) \cos(b_2) \end{bmatrix} \quad (2)$$

Based on the incident sun vector, two sun angles can be deduced as shown in Equations (3) and (4). These two sun angles which function as the truth-values are determined by the rotation of the rotary table.

$$\alpha_0 = -b_2 \quad (3)$$

$$\beta_0 = \arctan \frac{\tan(b_1)}{\cos(b_2)} \quad (4)$$

In coordinate  $X_b Y_b Z_b$ , the original point is the center of the sun spot obtained in the image plane when the incident sunray which goes through the pinhole  $(0, 0, h)$  on the mask is perpendicular to the image plane. After the initial calibration process of the DSS during which the rotary table is adjusted to get the incident sunray perpendicular to the image

plane, the center of the actual sun spot obtained on the image plane is  $(dx, dy)$ , which introduces the principal point error. In such case, the initial sun vector with this kind of intrinsic parameter error can be expressed as follows:

$$\vec{S}_{b0} = \begin{bmatrix} dx \\ dy \\ -h \end{bmatrix}$$

Furthermore, there are extrinsic parameter error between coordinates  $X_a Y_a Z_a$  and  $X_b Y_b Z_b$  due to installation error. We assume that coordinate  $X_b Y_b Z_b$  is rotated from coordinate  $X_a Y_a Z_a$  by the order of  $zxy$  with the angle parameter of  $(c_1, c_2, c_3)$ .

The sun vector in coordinate  $X_b Y_b Z_b$  with both intrinsic and extrinsic parameter errors when the rotary table is at its initial status can be expressed by Equation (6):

$$\vec{S}_b = \begin{bmatrix} S_x \\ S_y \\ S_z \end{bmatrix} = C_{bc} C_{ca} C_{ba}^{-1} \vec{S}_{b0} = \begin{bmatrix} f_1(dx, dy, h, b_1, b_2, c_1, c_2, c_3) \\ f_2(dx, dy, h, b_1, b_2, c_1, c_2, c_3) \\ f_3(dx, dy, h, b_1, b_2, c_1, c_2, c_3) \end{bmatrix} \quad (6)$$

Moreover, given the refraction error with correction coefficient  $k^{[6]}$ , which is related to the material of the cover glass of the image detector, the thickness of the cover glass and the distance between the image detector and the mask ( $h$ ), the theoretical center of the sun spot obtained in the image plane is determined by Equations (7) and (8):

$$x'_i = h_1(dx, dy, h, b_1, b_2, c_1, c_2, c_3, k) \quad (7)$$

$$y'_i = h_2(dx, dy, h, b_1, b_2, c_1, c_2, c_3, k) \quad (8)$$

Thus, the theoretical sun angles can be calculated by Equation (9) and (10):

$$\alpha_m = \arctan \left( \frac{x'_i - dx}{h - dh} \right) = g_1(dx, dy, dh, b_1, b_2, c_1, c_2, c_3, k, h) \quad (9)$$

$$\beta_m = \arctan \left( \frac{y'_i - dy}{h - dh} \right) = g_2(dx, dy, dh, b_1, b_2, c_1, c_2, c_3, k, h) \quad (10)$$

Where,  $dh$  is the height error between the image detector plane and the mask plane, which is associated with the mechanical processing accuracy and is another intrinsic parameter error. Therefore, given

the position of the sun spot we obtained in the image detector, the Equations (9) and (10) provide a method to calculate and analyze the incident angle with all intrinsic parameter error, extrinsic parameter error and refraction error taken into account.

The fundamental calculation method for measurement error simulation is expressed through Equations (11) and (12):

$$\alpha_{error} = \alpha_m - \alpha_0 \quad (11)$$

$$\beta_{error} = \beta_m - \beta_0 \quad (12)$$

### 3 Measurement error simulation analysis and discussion

Based on the system modeling and Equations (11) and (12), the measurement error of the digital sun sensors with respect to different error sources can be analyzed through numerical simulations.

As shown in Fig.2, the measurement error caused by the intrinsic parameter  $dh$  is applied to both incident angles with the same tendency. Take the measurement error of incident angle  $\alpha$  for example, it is only relevant to the value of input  $\alpha$  and it will increase to a maximum before it begins to decrease with the increase of the absolute value of input  $\alpha$ .

As for the measurement error caused by the intrinsic parameter  $dx$  or  $dy$ , the result of the numerical simulations, shown in Fig. 3, indicates that,  $dx$ , the principal point error in X direction leads to the measurement error of both  $\alpha$  and  $\beta$ ; on the other

hand,  $dy$ , the principal point error in Y direction only results in the measurement error of  $\beta$  which is the component of incident sunray in Y direction while it introduces no measurement error of  $\alpha$ , which is the component of incident sunray in X direction. Moreover, similar to the measurement error of  $\alpha$  caused by  $dx$ , the measurement error of  $\beta$  caused by  $dy$  is less in the center FOV than it in the edge of FOV.

Since the goal of accuracy of our DSS is arc-second level, the extrinsic parameter error is set to be  $10''$ . Thus, the simulation results of measurement error introduced by installation error in all three axes are shown in Fig. 4.  $c_1$  and  $c_2$  are the installation error introduced by rotation around X and Y axis, separately while  $c_3$  is the installation error introduced by rotation around the principal axis, which is perpendicular to the X-Y plane. Overall, the measurement error in the center FOV is negligibly small while it would significantly increase when the angle of the incident sunray increases at certain direction. Based on further analysis, the pattern of measurement error of  $\alpha$  caused by  $c_1$  is similar to the pattern of measurement error of  $\beta$  caused by  $c_2$  while the pattern of measurement error of  $\alpha$  caused by  $c_2$  is similar to the pattern of measurement error of  $\beta$  caused by  $c_1$ . And the pattern of measurement error of  $\alpha$  caused by  $c_3$  is similar to the pattern of measurement error of  $\beta$  caused by  $c_3$ .

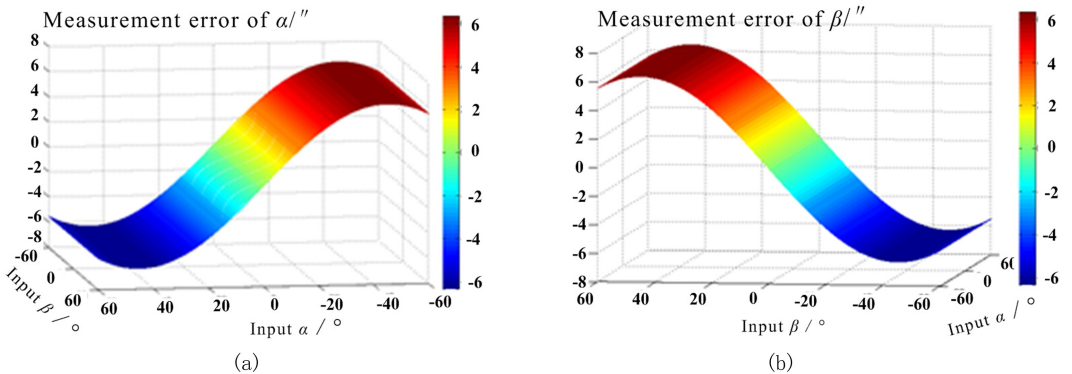
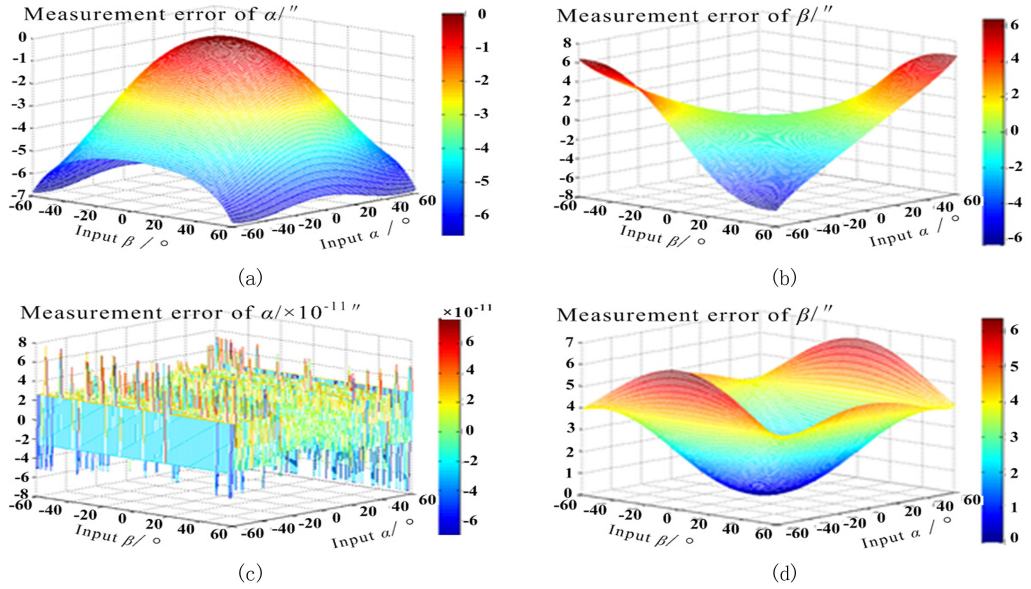
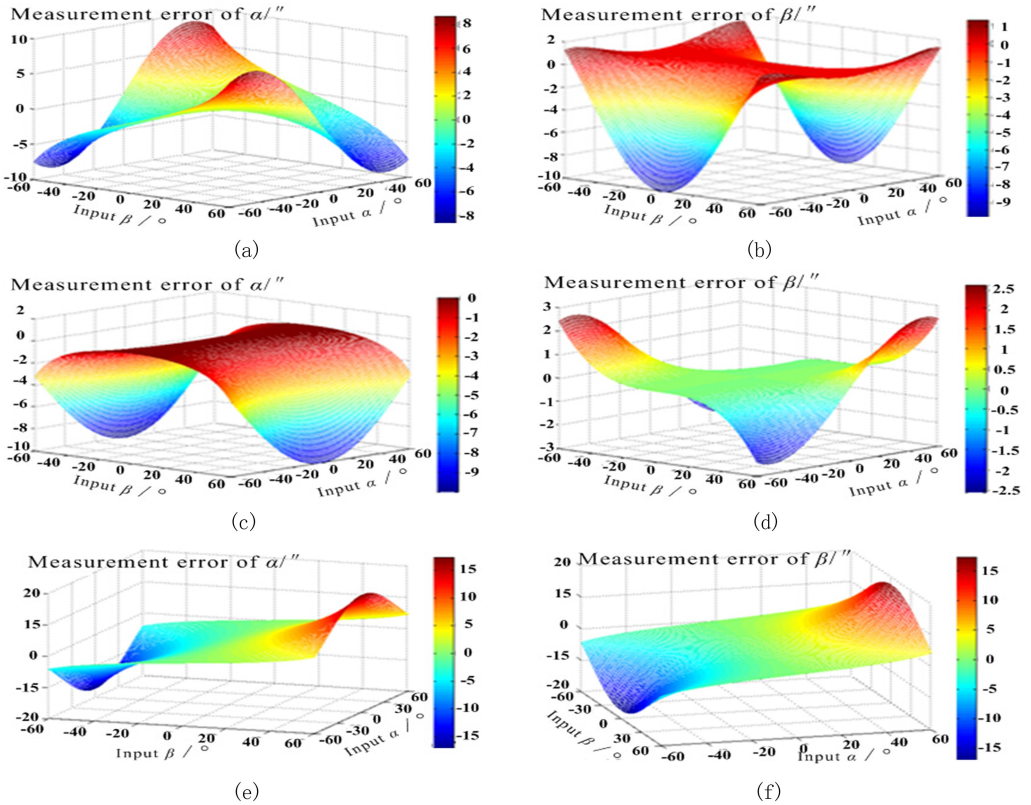


Fig. 2 Measurement error caused by intrinsic parameter error with  $dh = 0.2$  pixel.

(a) measurement error of  $\alpha$ , (b) measurement error of  $\beta$



**Fig. 3** Measurement error caused by the principal point error. (a) measurement error of  $\alpha$  with  $dx = 0.1$  pixel, (b) measurement error of  $\beta$  with  $dx = 0.1$  pixel, (c) measurement error of  $\alpha$  with  $dy = 0.1$  pixel, (d) measurement error of  $\beta$  with  $dy = 0.1$  pixel



**Fig. 4** Measurement error caused by the extrinsic parameter error. (a) measurement error of  $\alpha$  with  $c_1 = 10''$ , (b) measurement error of  $\beta$  with  $c_1 = 10''$ , (c) measurement error of  $\alpha$  with  $c_2 = 10''$ , (d) measurement error of  $\beta$  with  $c_2 = 10''$ , (e) measurement error of  $\alpha$  with  $c_3 = 10''$ , (f) measurement error of  $\beta$  with  $c_3 = 10''$

For a group of specific design parameters<sup>[6]</sup>, the simulation result of the measurement error caused by the refraction is revealed in Fig. 5. Due to the refraction when light goes through the cover glass of the image detector, the measurement error of  $\alpha$  will

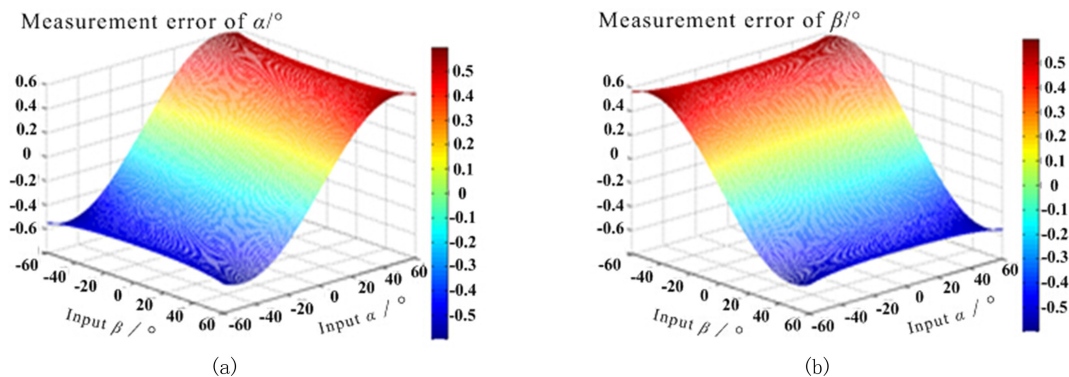


Fig. 5 Measurement error caused by the refraction. (a) measurement error of  $\alpha$ , (b) measurement error of  $\beta$

Based on the equations and simulation results, it is obvious that the measurement errors from different error sources were coupled and it is hard to decouple a single error source from others. The conventional methods to calibrate a DSS mainly include polynomial fitting, least square estimation and neural networks<sup>[11, 12]</sup>. However, none of them could uncover the actual influence of all the error sources on the system accuracy since the intrinsic and extrinsic parameter errors were treated together in all the mentioned methods, and the refraction error was overlooked. Under such circumstances, all the three kinds of error sources which were discussed and analyzed in this work should be considered to calibrate a DSS with high accuracy and some available optical measurement methods with high precision should be employed to improve the system calibration result together with the conventional error compensation method<sup>[7]</sup>.

## 4 Conclusion

A system modeling has been built and a theoretical method for measurement error analysis has proposed and derived in this work. The measurement error with respect to intrinsic parameter error, extrinsic parameter error and refraction error has been ana-

lyzed respectively and the simulation results indicated that the patterns of measurement error resulted from different error sources are distinct and the system accuracy was influenced by all different error sources synthetically. Thus, to achieve a DSS with extra-high accuracy, all the error sources should be considered when the whole system is calibrated.

## ACKNOWLEDGMENT

This work has been carried out in the State Key Laboratory of Precision Instrument Measurement, Tsinghua University under the financial support by the National 863 Project (No. 2012AA121503), the China NSF projects (No. 61377012, No. 61505094) and China Postdoctoral Science Foundation funded project (2015M571034).

## References

- [1] GIANCARLO R, MICHELE G. Multi-Aperture CMOS Sun Sensor for Microsatellite Attitude Determination[J]. Sensors, 2009, 9(6):4503-4524.
- [2] WEI M, XING F, YOU Z, et al. Multiplexing image detector method for digital sun sensors with arc-second class accuracy and large FOV [J]. Optics Express, 2014, 22(19):23094-23107.
- [3] DE BOOM C W, LEIJTENS J A P, V. DUIVENBODE L M H, et al. Micro Digital Sun Sensor; Sys-

- tem in a Package [C]. MEMS, NANO, and Smart Systems, International Conference on IEEE Computer Society, 2004:322-328.
- [4] BAUER F H AND DELLINGER W. Gyroless fine pointing on small explorer spacecraft [C]. in Proceedings of the AIAA Guidance, Navigation and Control Conference, (American Institute of Aeronautics and Astronautics, Monterey, CA, 1993), 492-506.
- [5] WEI M S, XING F, LI B, et al. Investigation of Digital Sun Sensor Technology with an N-Shaped Slit Mask [J]. Sensors, 2011, 11(10):9764-9777.
- [6] WEI M S, XING F, LI B, et al. Investigation of Digital Sun Sensor Technology with an N-Shaped Slit Mask [J]. Sensors, 2011, 11(10):9764-9777.
- [7] WEI M, XING F, AND YOU Z. An implementation method based on ERS imaging mode for sun sensor with 1 kHz update rate and 1" precision level [J]. Optics Express, 2013, 21(26):32524-32533.
- [8] YU C, JIA J, LV Z, ET AL. Error analysis and compensation for CCD sun sensor [J]. Aerospace control, 2006, 24(4): 35-37.
- [9] ALVI B, ABBAS N, ISRAR A, et al. Optimized Design of Sun Sensor and Centroid Algorithm for Small Satellite Mission [C]. Wireless Communications, Vehicular Technology, Information Theory and Aerospace & Electronic Systems (VITAE), 2014 4th International Conference on IEEE, 2014:1 - 4.
- [10] STRIETZEL R. Two-dimensional calibration of a sun attitude sensor [C]. in Proceedings of the 15th International Federation of Automatic Control Triennial World Congress on Automatic Control, (IFAC, Barcelona, 2002), 259-264.
- [11] RUFINO G, PERROTTA A and GRASSI M. Laboratory test of an APS-based sun sensor prototype [C]. in Proceedings of the 5th International Conference on Space Optics, (ESA, Toulouse, 2004), 551-558.
- [12] TU B, HAN K, WANG H, et al. Design of digital sun sensor with large field [J]. Chinese Journal of Sensors and Actuators, 2011, 24(3): 336-341.

## Authors' Biographies



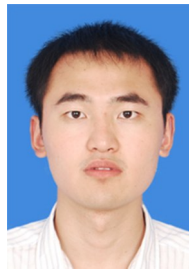
**WEI Minsong**, born in 1986, is currently a postdoctoral fellow in the Department of Precision Instrument, Tsinghua University, China. He obtained his Ph.D degree from Tsinghua University in 2014. His research interests include optical sensors and the performance improvement technology, etc.

Email: minsongwei@mail.tsinghua.edu.cn



**XING Fei**, born in 1979, is currently an associate professor in Tsinghua University, China. He received his Bachelor degree from Tongji University in 2002 and Ph.D. degree from Tsinghua University in 2007. His current research interests focus on advance optical attitude sensor for space, remote sensing and celestial navigation.

Email: xingfei@tsinghua.edu.cn



**WANG Geng**, born in 1988, is currently a Ph.D candidate in the Department of Precision Instrument, Tsinghua University, China. His major interests include high accuracy sun sensor and star tracker technology, etc.

Email: wanggeng1210@sina.com



**YOU Zheng**, born in 1963, is an Academician of Chinese Academy of Engineering, and a Professor of Chang Jiang Scholar in Tsinghua University, China. He is also the Assistant President of Tsinghua University, the Dean of the School of Mechanical Engineering and the Chairman of the Department Precision Instrument.

Respectively. His current research includes MNT technology, Micro/Nano satellite technology and their applications

Email: yz-dpi@tsinghua.edu.cn